

*Analysis of Unabsorbed Light from Exploding-Pusher Targets Used for Proton Backlighting on  
the National Ignition Facility*

**Phoebe Huang**

Webster Schroeder High School

Advisor: Dr. R. S. Craxton

Laboratory for Laser Energetics

University of Rochester

Rochester, New York

March 2016

## 1. Abstract

There is substantial interest in proton backlighting on the National Ignition Facility (NIF), requiring a small number of beams to be pointed at a secondary backlighter target (a thin shell containing  $D^3He$  that produces a burst of protons when it implodes) while a larger number irradiate a primary target. The protons provide a diagnostic of the primary target by being deflected or absorbed as they pass through it. Optimized designs for different size proton backlighter targets, using 32 of the 192 NIF beams, have been developed using the hydrodynamics simulation code SAGE. Small targets are desirable for producing a small proton source size. In all cases, the phase plates (optics that set a large beam size at best focus) are assumed to remain in the system (to avoid the time that would be required to remove them for the backlighter beams). It was found, as expected, that the amount of scattered light (unabsorbed laser energy that can pass through the target chamber and damage laser optics on the opposing side) increases as the target diameter decreases from 1500 to 420 microns. Adjustments were made to include the known scaling of optics damage with laser pulse length. These simulations explore the limits of what the NIF can safely shoot.

## 2. Introduction

As the world attempts to move away from fossil fuels and other nonrenewable energy sources, clean energy has become an important topic of research. One developing source of potential clean energy is nuclear fusion. Nuclear fusion can be achieved by irradiating a small, spherical target, consisting of a plastic or glass shell filled with tritium and deuterium, with laser beams. During irradiation, the shell of the target ablates outwards, forcing the fuel inside to be compressed. The compressed fuel reaches high density, pressure, and temperature, allowing for fusion reactions to take place. The extreme conditions are necessary for the deuterium and tritium, both positively charged nuclei, to overcome Coulomb repulsion forces and fuse before the target completely explodes. The fusion of deuterium and tritium produces a helium nucleus and an energetic neutron, the latter carrying most of the energy from the fusion reaction. In a perfect setting, the helium nucleus would redeposit its energy into the fuel and create a chain reaction of fusions in a process called ignition. Ignition is the first step in reaching breakeven, where the energy released by the reaction equals the energy put in by the laser. After breakeven has been achieved, the next goal is high gain, where the energy released by fusion is substantially more than the energy put in by the lasers. To make nuclear fusion into a plausible source of clean energy, high gain must be achieved.

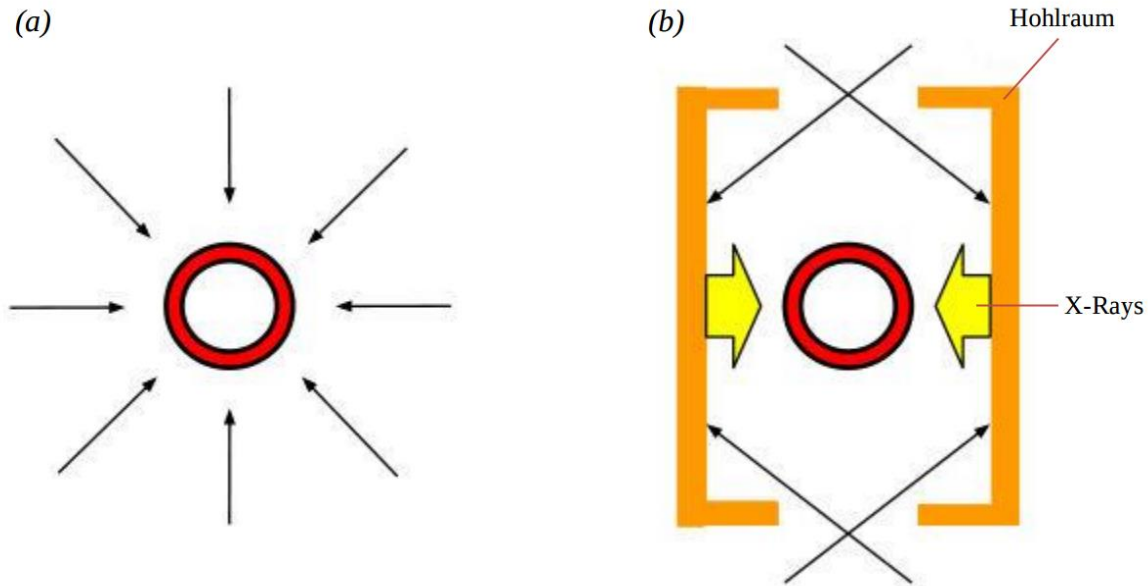


**Figure 1:** The two main approaches to inertial confinement fusion (ICF). (a) In direct drive, the lasers are aimed directly at the target. (b) In indirect drive, the lasers are aimed at the hohlraum, which emit x rays that then irradiate the target. (From Reference 3)

Currently, there are two main approaches used for laser fusion: direct drive<sup>1</sup> and indirect drive.<sup>2</sup> In direct drive Figure 1a, the lasers are aimed at the target and the target is irradiated directly by the laser beams. In indirect drive Figure 1b, lasers are pointed at the inner walls of a hohlraum, usually made of a metal with a high atomic number, so that the target can be irradiated by the x rays emitted by the hohlraum. The Omega laser at the Laboratory of Laser Energetics (LLE) is configured for direct drive, while the National Ignition Facility (NIF) at the Lawrence Livermore National Laboratory is configured for indirect drive. Indirect drive offers better uniformity of the implosion because the target is being irradiated more evenly by the x rays. However, 80% of the energy from the laser beams is either lost in the walls of the hohlraum or escapes through the openings of the hohlraum. The target only absorbs 20% of the energy originally provided.

Even though the NIF is configured for indirect drive, it can be adjusted to perform direct drive by repointing the beams in a method called polar drive. The NIF has a total of 48 beam ports, all evenly spaced around the azimuth ( $\Phi$ ) in 8 rows at angles of  $\Theta = 23.5^\circ, 30.0^\circ, 44.5^\circ,$  and  $50.0^\circ$  from the poles on the top and bottom. The lasers are grouped into quads, consisting of 4 beams; in total the NIF has 48 quads, or 192 beams. In polar drive, the beams are pointed away from the poles and towards the equator to make up for the lack of ports there, as illustrated in Figure 2.

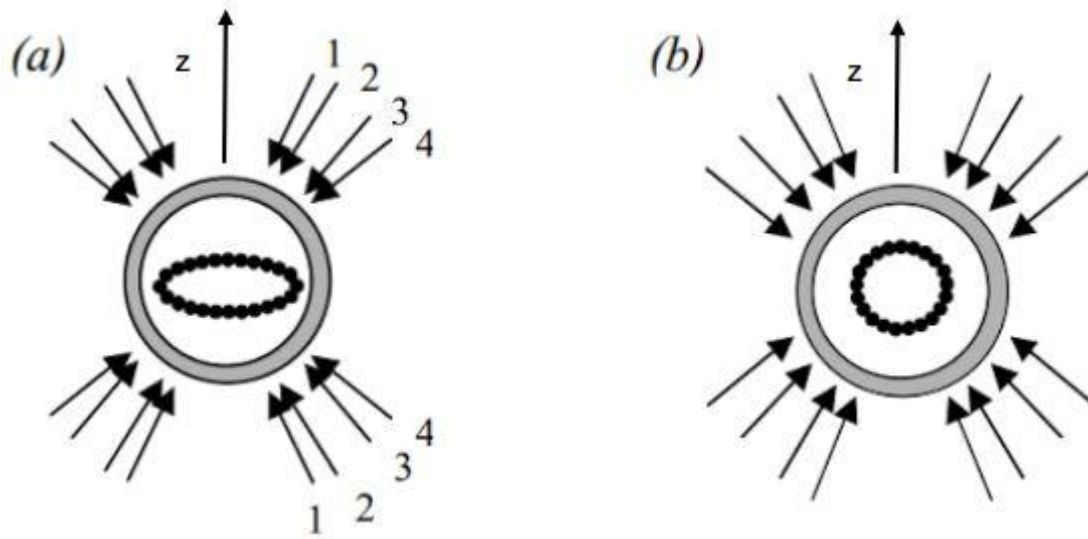


**Figure 2:** Direct drive beam pointings on the NIF. Each arrow represents a ring of quads. (a) With the beams aimed at the center of the target, the deposited energy is unevenly spread. The result is a much faster implosion at the poles than at the equator. (b) Repointing the beams towards the equator for the polar drive approach spreads out the energy more evenly, allowing for a much more uniform implosion. Based on Fig. 2 of Ref. 4

Using polar drive has been effective in creating uniform implosions during direct drive experiments on the NIF carried out by LLE.<sup>5</sup> It is also being used on the NIF<sup>6</sup> for the development of proton backlighting, a diagnostic technique illustrated in Figure 3. The backlighter and primary target are irradiated with different groups of laser beams. The

backlighter releases protons, which are deflected by the magnetic and electric fields of the primary target, hit a detector, and produce an image.

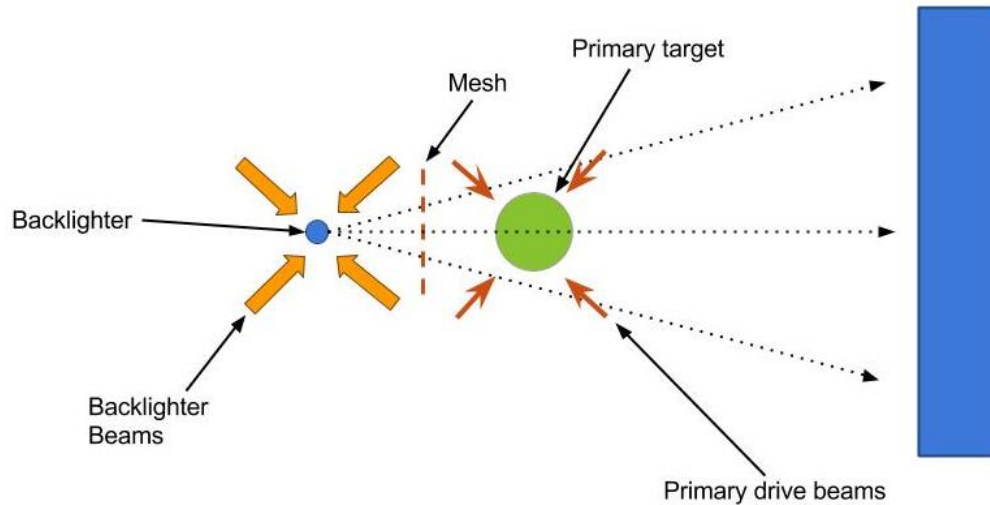


**Figure 3:** The proton backlighter, represented by the blue circle, sits behind the primary target, the green circle. A few beams are reserved for the backlighter, while most are pointed at the primary target. The backlighter beams irradiate the backlighter target directly, and release protons (dotted lines) that will produce an image providing information about the magnetic and electric fields of the primary target.

This project focused on the proton backlighter. The backlighter target in this project has a thin plastic shell, 4 microns thick, and is filled with a deuterium and helium-3 fuel. A small proton backlighter is desirable because a smaller point source leads to higher quality, more focused images, but has the disadvantage that scattered light may damage the laser optics. This project entailed the optimization of several proton backlighter targets of varying sizes and the assessment of their safety. As most of the quads would be required to irradiate the primary target, only 8 quads were reserved for use on the backlighter: every other quad  $44.5^\circ$  from the poles.

Another restriction was that phase plates, optics placed in laser beams to increase their size, spread, and uniformity in the target plane as shown in Figure 4a, must be used. Removing the phase plates takes a lot of time, so if the backlighter can be used with phase plates left in, it

will save a lot of time and expense. Current direct drive implosion experiments on the NIF use the phase plates (designed for indirect drive) with appropriate repointings and defocusing as proposed by Cok et al.<sup>4,7</sup>

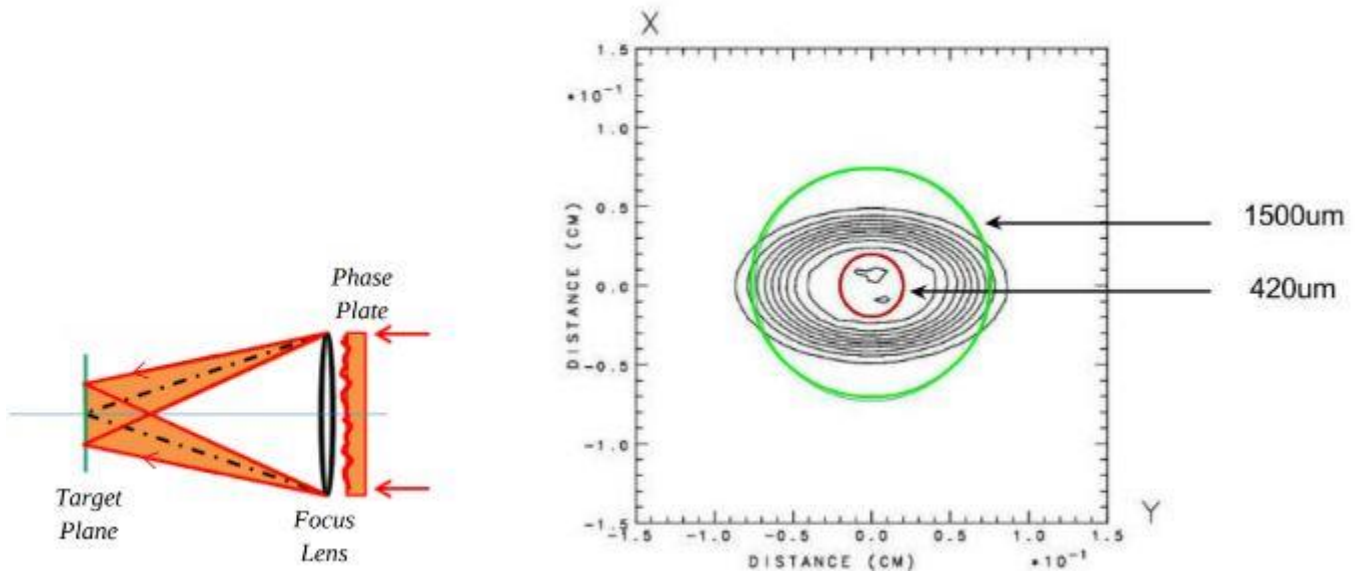


**Figure 4:** (a) Phase plates increase the size and spread of a beam to increase uniformity in energy distribution in the target plane. (b) The dark, oval rings represent intensity contours of the laser beam. A target with a larger diameter, in green, covers more area and can absorb more energy from the pulse. The smaller target, in red, is not big enough to absorb much energy. Most of the beam blows by it on the sides. (Based on Fig. 11 of Ref. 3)

An ideal implosion has minimized amounts of scattered light, to prevent possible damage to laser optics on the opposite side of the target chamber, and maximized uniformity. Depending on the size of the target and on where the beams are repointed, different amounts of scattered light, or unabsorbed energy, are produced. This can be seen in Figure 5, which shows ray-trace plots for two different target sizes.

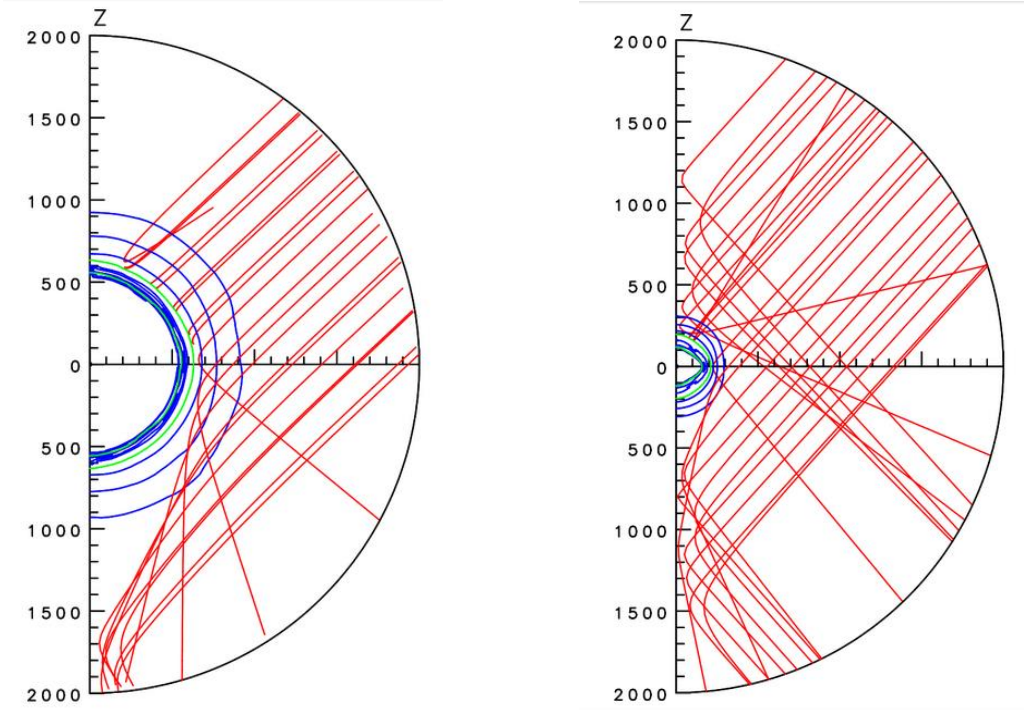


**Figure 5:** Ray trace diagrams show how the difference in size affects how each target absorbs energy. On the left is a 1500 micron target and on the right is a 420 micron target. The red lines represent the beams and the blue is the target. Notice that the beams are not aimed at the target center; this is a result of repointing for polar direct drive. The slant comes from the port angle. The 1500 micron target blocks most of the red rays, but the smaller target does not. The excess beam energy that is neither absorbed nor blocked becomes scattered light.

Scattered light is produced when not all the energy provided by the laser is absorbed by the target. Repointing beams can cause an increase in scattered light because many rays no longer point directly at the target and are not completely absorbed or blocked by it. Repointed beams give a better spread of energy and better uniformity because they cover more area. However, if scattered light increases too much, the design is not viable. Phase plates also increase the spread of a beam and contribute to better uniformity at the price of increased scattered light.

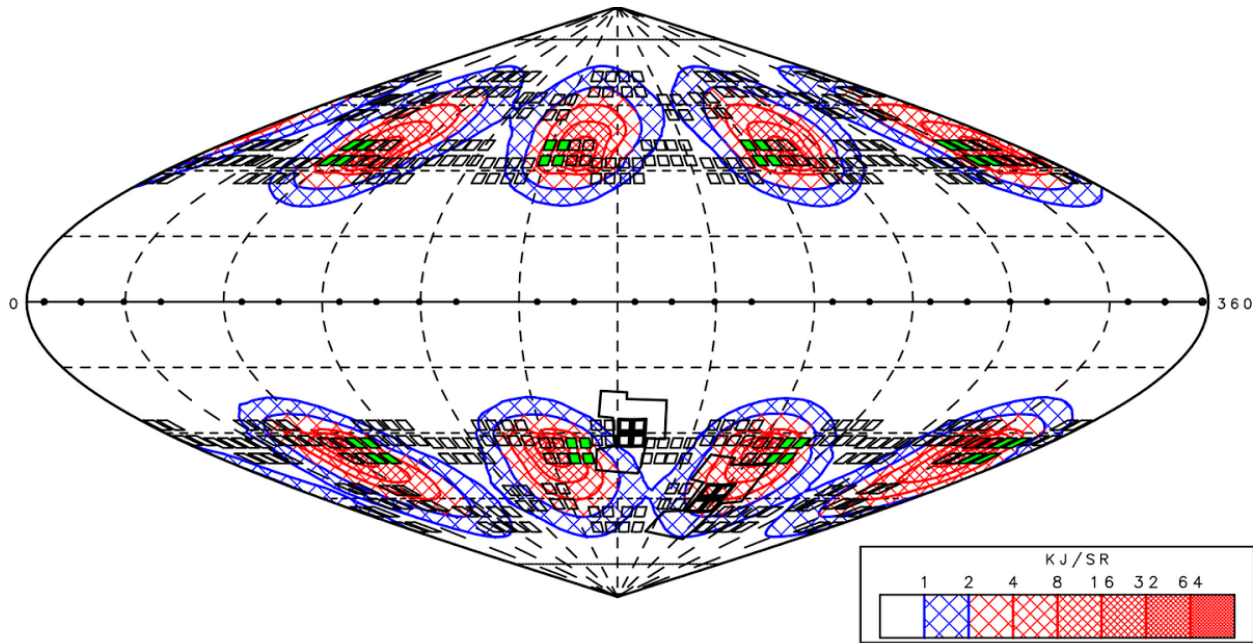


**Figure 6:** This scattered light contour plot shows where the excess energy from the beams is hitting. The red areas are where the most energy is concentrated, and blue is the least. The quads in green are the ones being used. The most concentrated red areas are extremely close to the green quads, indicating that much of the excess energy is hitting close to the ports being used on the opposite side of the target chamber.

Figure 6 gives a contour plot of the scattered light as a function of angle for a target with diameter 1000 microns. The regions of greatest scattered light lie very close to the beam ports being used (shown in green). The quads used are almost directly across from each other, and if too much excess energy gets into them, the mirrors in the laser beam path can be damaged. For each design, the maximum scattered light at any angle was used to assess the damage risk.

### 3. Simulation results

An optimized design for a 1500  $\mu\text{m}$  diameter target developed by Garcia<sup>8</sup> was used as the starting point for data collecting and was the only 1500  $\mu\text{m}$  diameter target analyzed. Optimized designs for targets of 1000, 800, 600, and 420 micron diameters were created by varying the beam position, focus, and pulse length. The designs were optimized for good uniformity. Three

designs with best uniformity at each target size were typically chosen and their amounts of scattered light graphed.

Optimization of targets proceeded in descending order of their diameters. For each new target size, the first two runs used Garcia's design and the design with best uniformity from the previous design to provide starting points for the optimization. In the case of the 1000 micron diameter target, just Garcia's design was used as the starting point. For the 1500 micron diameter target, Garcia's design produced a nonuniformity of 1.53% and a maximum scattered light flux of 31.6 kJ/sr up to the time of peak implosion, equivalent to  $0.05 \text{ J/cm}^2$  on the laser optics. An example of a design optimized for uniformity is given in Figure 7, which shows contours of the center-of-mass radius for a 1000-micron target. The poles and equator were significantly underdriven in the starting design, so in the optimized designs [Figure 7], three out of the four beams in each quad were pulled towards the equator and the remaining one was aimed closer to the pole. This provided a much better uniformity.

The original plan was to use best focus for all the designs to reduce the amount of scattered light by as much as possible, but it was found that with defocus, the amount of scattered light did not increase by too significant of an amount but uniformity improved. Defocusing the beam increases its spread. The best design created for the 1000 micron target had a nonuniformity of 1.82% and produced 54.3 kJ/sr of scattered light at its time of peak implosion. The same method was used for optimizing the 800 and 600 micron diameter targets, which had similar designs to the optimized 1000 micron diameter target. The best design for the 800 micron diameter target produced a nonuniformity of 4.11% and 59.8 kJ/sr of scattered light. The best design for the 600 micron diameter target produced 5.64% nonuniformity and 73.0 kJ/sr of scattered light.

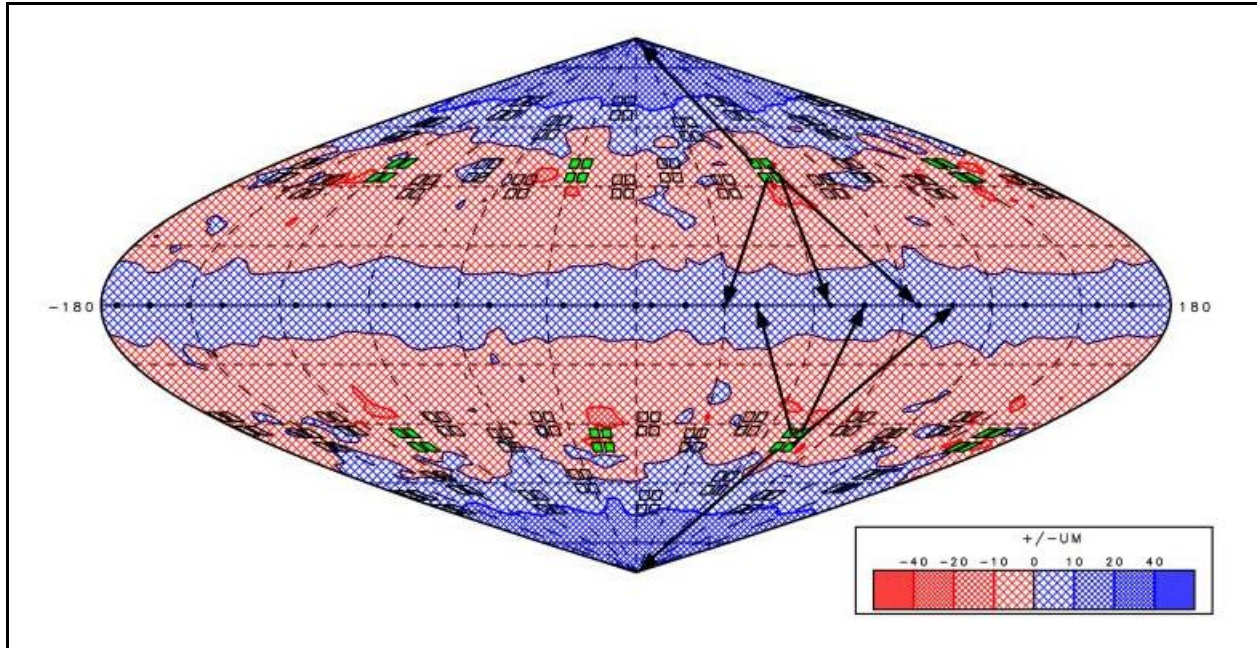


**Figure 7:** Contour plot of deviation in the center-of-mass radius of the imploding shell when the shell has imploded approximately half way, on a sinusoidal projection of a 1000 micron target, showing the entire surface. The green quads are the ones in use and the black arrows show where each beam of a quad is pointed in an optimized design. Red areas are overdriven and blue areas are underdriven. Variations of this design were tested with different beam defocuses to achieve a better uniformity but with a minimal increase in scattered light. The optimized designs for the smaller targets were very similarly structured.

Simulations for the 420 micron diameter target began the same way as the others, but it was found that the target was imploding before the beam had reached full power. Therefore, the length of the beam was changed from 2.1 ns to 1.1 ns and the time to reach full power was decreased from 1.0 ns to 0.2 ns. The thickness of the shell was also changed from 4 microns to 2 microns. The optimized design had a nonuniformity of 5.62% and produced 83.9 kJ/sr of scattered light.

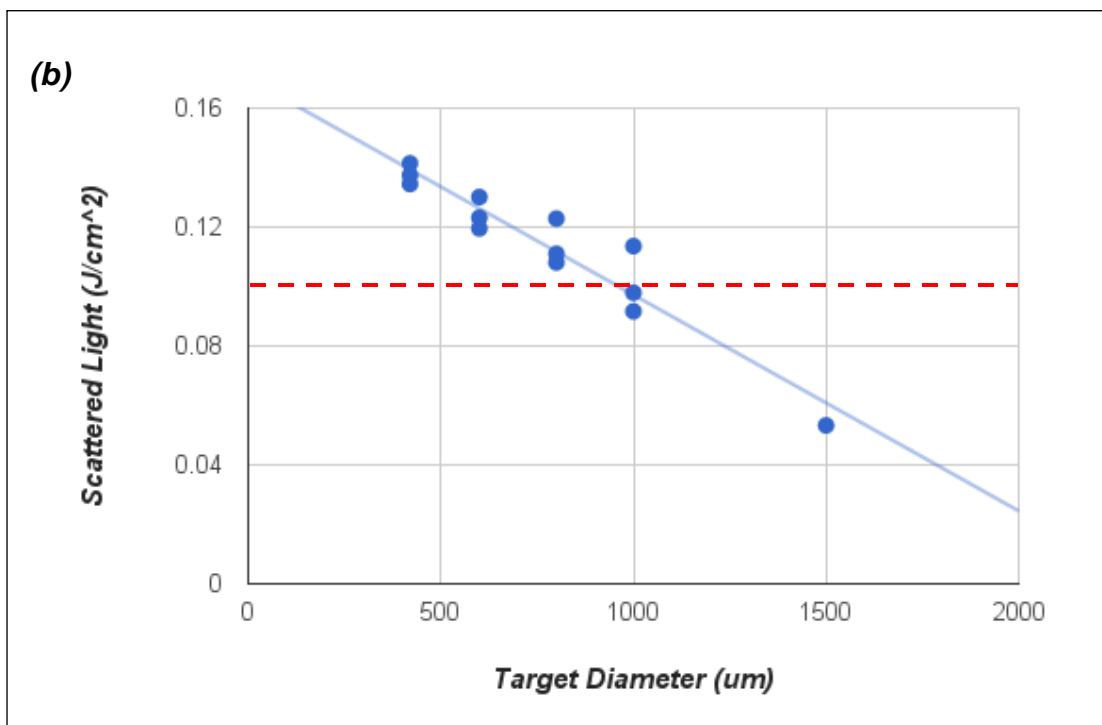
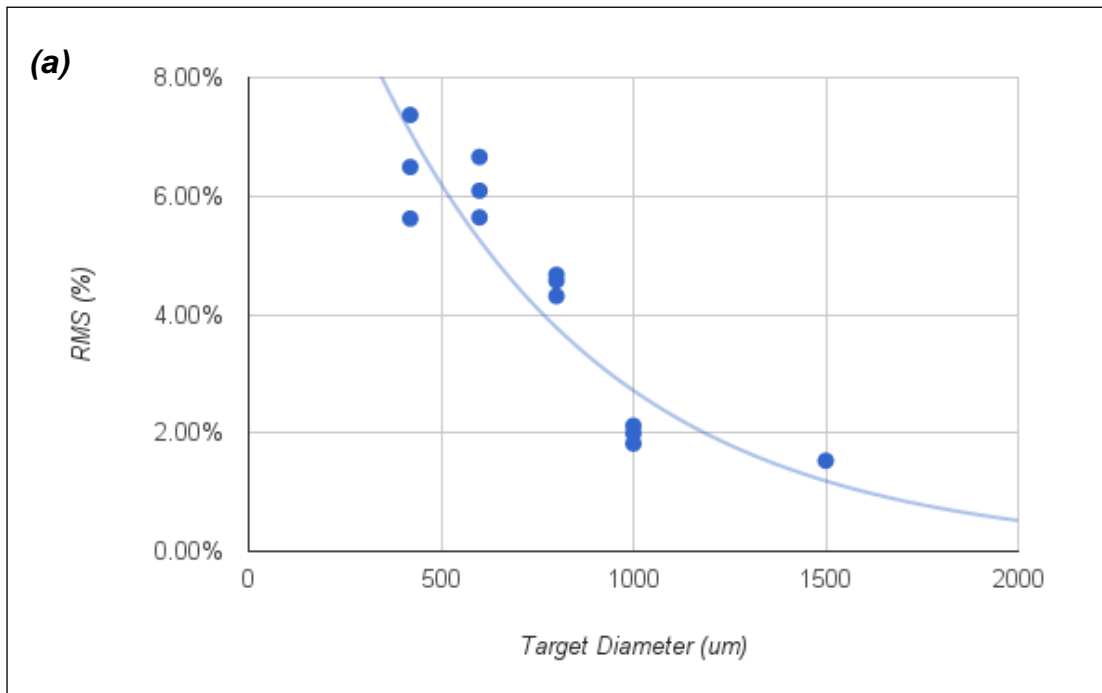


**Figure 8:** Graph (a) is of uniformity vs target diameter for the best designs. Graph (b) is of the amount of scattered light produced by the same designs vs the target diameter. As the target size gets larger, the nonuniformity and amount of scattered light decrease. The red dotted line at  $0.10 \text{ J/cm}^2$  represents the level of scattered light considered safe.

Graphs of the nonuniformity and amount of scattered light for the best designs are shown in Figure 8. There is a clear trend: both nonuniformity and the amount of scattered light decrease when the target diameter increases. The 1500 micron target is definitely safe to shoot and two out of the three optimized 1000 micron designs are safe. However, these results do not account for the short amount of time in which all the energy hits the mirrors. The same amount of force, applied in a short amount of time, will cause more damage than if it took a long time to completely expend its energy. To accommodate the short pulses, the amount of scattered light measured was converted to find their 5 ns equivalent. Dr. B. MacGowan from the Lawrence Livermore National Laboratory provided the conversion equation:<sup>9</sup>

$$F_{adj} = F(5 \text{ ns}/T)^{0.35}$$

where F is the flux on the mirror,  $F_{adj}$  is the flux adjusted to a 5-ns equivalent, and T is the length of the scattered light pulse.

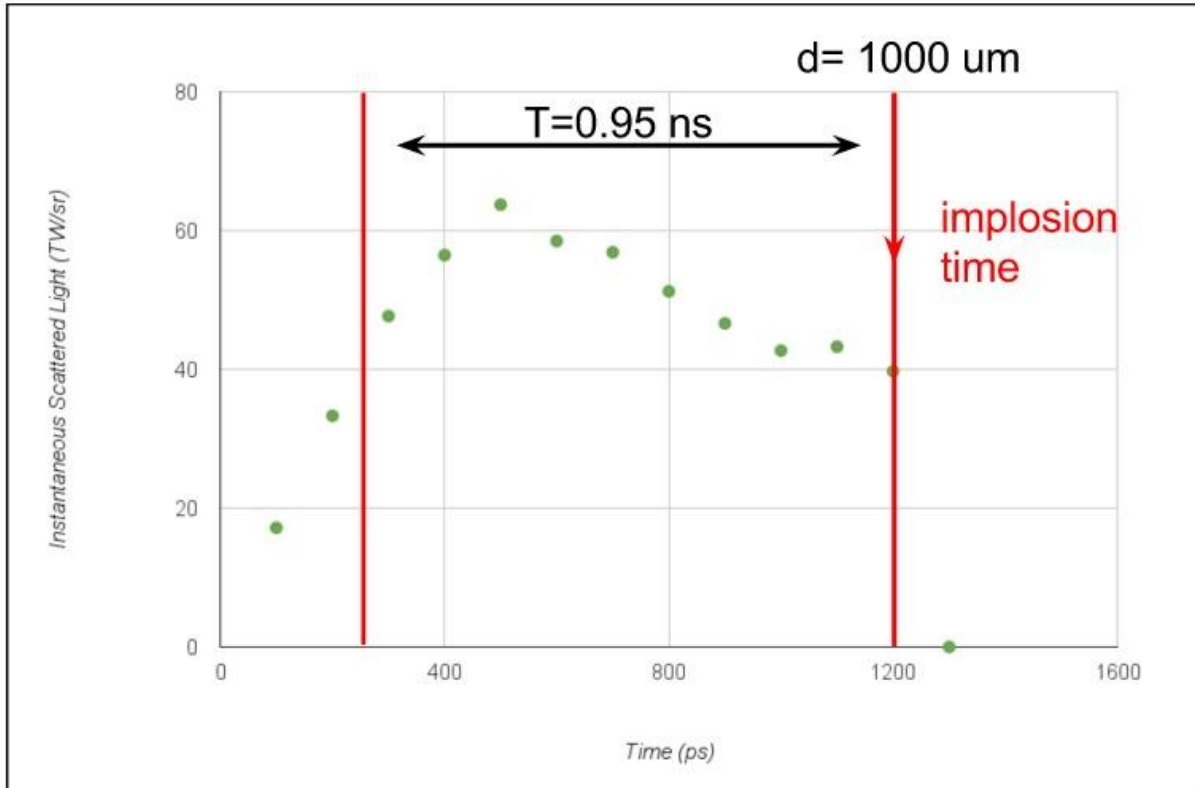


**Figure 9:** A plot of instantaneous scattered light vs time for a 1000 micron target. The red lines mark the beginning and the end of  $T$  (labeled by the black arrow).

To find  $T$ , the scattered light produced every 100 picoseconds was graphed, as shown in Figure 9, and from it the approximate  $T$  was obtained for every target size. The beginning of  $T$  was roughly halfway to the first peak in scattered light and the end of  $T$  was at the time of implosion. This method provides a more accurate estimate of  $T$  than simply taking the pulse length up to the implosion time (around which time the laser pulse would normally be shut off). Applying the formula gave the results shown in Table 1.

**Table 1.** Adjustment factor  $(5ns/T)^{0.35}$  for the various designs.

Diameter	Time (ns)	Factor
1500 um	1.35	1.58
1000 um	.95	1.79
800 um	.80	1.90
600 um	.75	1.94
420 um	.30	2.68

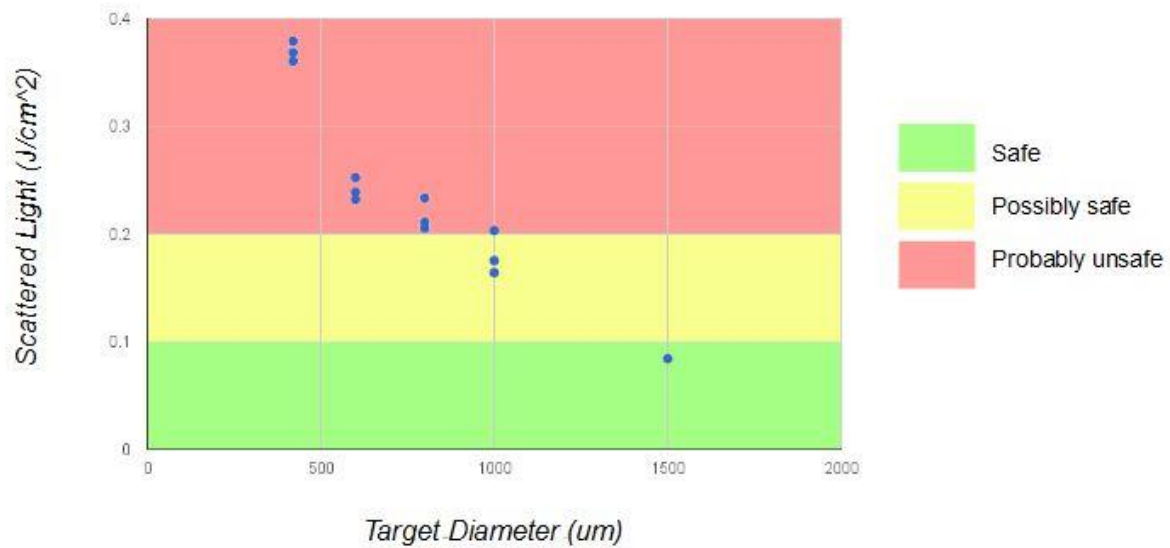


**Figure 10:** This graph is the same as Figure 9b, but with the scattered light fluxes adjusted to a 5-ns equivalent. The zones where the adjusted scattered light renders a shot safe (green), possibly safe (yellow), and unsafe (red) are shown. The only backlighters in the green zone are the 1500 micron ones. The 1000 micron targets fall mostly in the yellow zone. The 800, 600, and 420 micron targets all fall in the red zone.

Using the factors in Table 1, the scattered fluxes of Figure 8b were adjusted to provide more accurate estimates of what is safe to shoot [Figure 10]. The only target that is completely safe to shoot is the 1500 micron one. The 1000 micron target is borderline safe. Two designs for

this diameter are in the possibly safe zone, indicating that further tests will need to be done to determine their viability. The other design is in the unsafe zone, along with all the smaller target sizes.

#### **4. Conclusion**

The amount of scattered light produced in the implosion of proton backlighter targets has been investigated for targets of diameter ranging from 1500 microns to 420 microns. Accurate estimates of the scattered light are required because excessive light passing through beam ports on the opposite side of the NIF target chamber can damage laser optics. Since shorter pulses provide a greater risk to the optics for a given laser flux, the duration of the scattered light pulse was calculated for each target size and the flux was appropriately adjusted to an equivalent flux at 5 ns.

The amount of scattered light produced from 420 micron diameter targets is above the recommended and safe amount. It may be possible to use the backlighters deemed unsafe in this project if different beams are available for use and the ports on the opposite sides of the target chamber are blocked to prevent damage from scattered light. However, this would reduce the number of beams available to irradiate the primary target.

#### **5. Acknowledgements**

I would like to thank Dr. Craxton for showing me how to work with SAGE and helping me along with my project. Also, I would like to give a big thank you to Emma Garcia for giving me advice and helping solve my computer issues.

## 6. References

1. J. Nuckolls et al., “*Laser Compression of Matter to Super-High Densities: Thermonuclear (CTR) Applications,*” *Nature* **238**, 139 (1972).
2. J.D. Lindl, “*Development of the Indirect-Drive Approach to Inertial Confinement Fusion and the Target Basis for Ignition and Gain,*” *Phys. Plasmas* **2**, 3933 (1995).
3. Y. Kong, “*Beam-Pointing Optimization for Proton Backlighting on the NIF,*” Laboratory for Laser Energetics High School Summer Research Program (2013).
4. A.M. Cok, “*Development of Polar Direct Drive Designs for Initial NIF Targets,*” Laboratory for Laser Energetics High School Summer Research Program (2006).
5. P.B. Radha et al., “*Direct Drive: Simulations and Results from the National Ignition Facility,*” to be published in *Phys. Plasmas*.
6. J.R. Rygg et al., “*A Monoenergetic Proton Backlighter for the National Ignition Facility,*” *Rev. Sci. Instrum.* **86**, 116104 (2015).
7. A.M. Cok et al., “*Polar-Drive Designs for Optimizing Neutron Yields on the National Ignition Facility,*” *Phys. Plasmas* **15**, 082705 (2008).
8. E.M. Garcia, private communication (2015).
9. B.J. MacGowan, private communication (2015).